Two-step shell-model calculation of ^{208}Po†

William W. True
Physics Department, University of California, Davis, California 95616
and
Chin W. Ma
Physics Department, Indiana University, Bloomington, Indiana 47401
(Received 1 October 1973)

The low-lying levels ^{208}Po have been calculated by a two-step shell-model calculation which uses the vector-coupled states from ^{206}Pb and ^{210}Po as a basis. The calculated and experimental energy levels are in good agreement with each other.

[NUCLEAR STRUCTURE ^{208}Po; two-step shell model, calculated levels, J,π.]

I. INTRODUCTION

Conventional shell-model calculations have been able to correlate and explain in a systematic manner a great deal of the experimental data in the lead region. For example, the recent calculations by Ma and True[1] have been able to describe the structure and positions of most of the low-lying levels in the eight nuclei ^{206}Pb, ^{210}Pb, ^{210}Po, ^{208}Bi, ^{210}Bi, ^{208}Tl, ^{206}Tl, and ^{206}Hg.

By using the results of the calculations of Ma and True for the nuclei ^{206}Pb and ^{210}Po, it is possible to construct a suitably truncated basis which can be used to describe the structure of the low-lying levels of ^{208}Po. The motivation for using a two-step approach and expressions for the two-hole–two-particle matrix elements will be described in Sec. II. Section III will discuss the ^{208}Po calculations and compare the results with the experimentally observed data.

II. THEORY

A. Basis states

From a conventional shell-model viewpoint, ^{208}Po should be described by two proton particles outside of and two neutron holes in the doubly magic nucleus ^{208}Pb. In this paper, the neutron holes will be restricted to orbitals in the major neutron shell just below $N=126$ and the proton particles will be restricted to orbitals in the major proton shell just above $Z=82$ and these orbitals[2] are shown in Fig. 1. The justification for neglecting other possible single-particle orbitals is the relatively large energy gaps between major shells. On the other hand, there is usually no *a priori* reason why some orbitals in a major shell should be used while others are neglected. In fact, calculations indicate that all orbitals in a major shell should be retained since important correlations result from configuration mixing—see for example, the Ma and True calculations.[1]

A conventional shell-model calculation for ^{208}Po would be to diagonalize the Hamiltonian matrix where the basis states consist of coupling two holes and two particles to a given total angular momentum J. Restricting the neutron holes and proton particles to the orbitals between the magic numbers of 82 and 126, there will be about 2500 basis states for $J=2^+$ in ^{208}Po. Although not impossible, it is not feasible with present day computers to evaluate and diagonalize the resulting 2500 by 2500 $J=2^+$ Hamiltonian matrix. An alternative approach, which is used in this paper, is to do a two-step shell-model calculation where a set of correlated basis states are used which contain the important correlations between particles or holes in a major shell and where a suitable truncation can be made such that the Hamiltonian matrices to be diagonalized are not large.

The uncorrelated ^{208}Pb ground state will be taken as the "vacuum" state or "core," and creation and annihilation operators for particles and holes are defined relative to this core. The Hamiltonian can be written symbolically as

$$H = H_C + H_{Cp} + H_{Ch} + V_{pppp} + V_{hhhh} + V_{hphp} + V' . \quad (1)$$

In Eq. (1), H_C represents the Hamiltonian of the core consisting of the kinetic energies and mutual interaction energies of all the particles in the core. The eigenvalue E_C of H_C is a constant energy which will not be considered further since all energies will be renormalized so that the ground state of ^{208}Po will lie at zero energy.

H_{Cp} is the core-particle Hamiltonian representing the kinetic energy of the particles outside the core plus their interaction with the particles in the core while H_{Ch} describes the holes in a similar fashion.

V_{hhhh}, V_{pppp}, and V_{hphp} represent the hole-hole,

particle-particle, and hole-particle interactions, respectively. V' represents everything else in the Hamiltonian and will be neglected from now on since V' will not contribute to the Hamiltonian matrix elements when the basis consists of two-hole–two-particle states.

In the conventional shell-model calculation described above, the basis states are eigenfunctions of $H_{cp}+H_{ch}$. One would then calculate the matrix elements of $V_{pppp}+V_{hhhh}+V_{hphp}$ and diagonalize the resulting Hamiltonian matrix. However, as was pointed out above, this approach is not feasible as very large matrices would be encountered.

An alternative approach, the two-step shell-model approach, is to form a set of correlated basis states by vector coupling the eigenfunctions of $H_{cp}+V_{pppp}$ to the eigenfunctions of $H_{ch}+V_{hhhh}$ and then diagonalizing the interaction V_{hphp}. For ^{208}Po, the eigenfunctions of $H_{cp}+V_{pppp}$ are the ^{210}Po eigenstates while the eigenfunctions of $H_{ch}+V_{hhhh}$ are the ^{206}Pb eigenstates. If all the allowed eigenstates of ^{210}Po and ^{206}Pb were used to construct a correlated basis for the second step in a two-step calculation, the matrices to be diagonalized would be just as large as for the conventional shell-model approach described above since both bases span the same configuration space. However, if energy considerations and/or some other criteria can be used to limit the number of eigenstates which are used from ^{210}Po and ^{206}Pb, then the number of basis states used in the second step of the two-step approach can be made relatively small. As will be seen in Sec. III below, only nine eigenstates from ^{206}Pb and five eigenstates from ^{210}Po were used in constructing a correlated basis for the ^{208}Po calculation.

It should be stressed, however, that the ^{206}Pb eigenstates will have neutron-hole correlations from the whole major neutron shell contained in them and similarly the proton-particle correlations from the major proton shell will be contained in the ^{210}Po wave functions. Providing the particle-hole interaction is not so strong as to significantly alter these correlations, the two-step approach will be valid. If, on the other hand, these correlations are significantly altered, then a larger basis will have to be used in the two-step calculation and the two-step approach may become just as "complicated" as a conventional shell-model approach. As will be discussed in Sec. III, the good agreement between the experimentally observed energy levels in ^{208}Po and those calculated by the two-step process implies that the hole-particle interaction does not drastically alter the correlations which are already present in the ^{206}Pb and ^{210}Po eigenfunctions.

For the two-step calculation to work, the eigenstates used to form the correlated basis should be "very good" eigenstates. For example, the eigenstates of ^{206}Pb and ^{210}Po used to construct the correlated basis for ^{208}Po should give very good descriptions of the low-lying states in ^{206}Pb and ^{210}Po, respectively. If this were not the case, then one would not expect to obtain a good description of the low-lying states in ^{208}Po.

In a two-step calculation where one vector couples two multiparticle eigenstates together, care must be taken to insure that all like particles are antisymmetrized and that center-of-mass spurious states are eliminated in the final results. Neither of these two problems arise for the two-step calculation of ^{208}Po. The neutron holes are already antisymmetrized in the ^{206}Pb wave functions and the proton particles are already antisymmetrized in the ^{210}Po wave functions. In general, there are no center-of-mass spurious state problems if one restricts oneself to a single harmonic-oscillator shell. In the ^{208}Po case, the major shell for neutron holes and proton particles differ from the

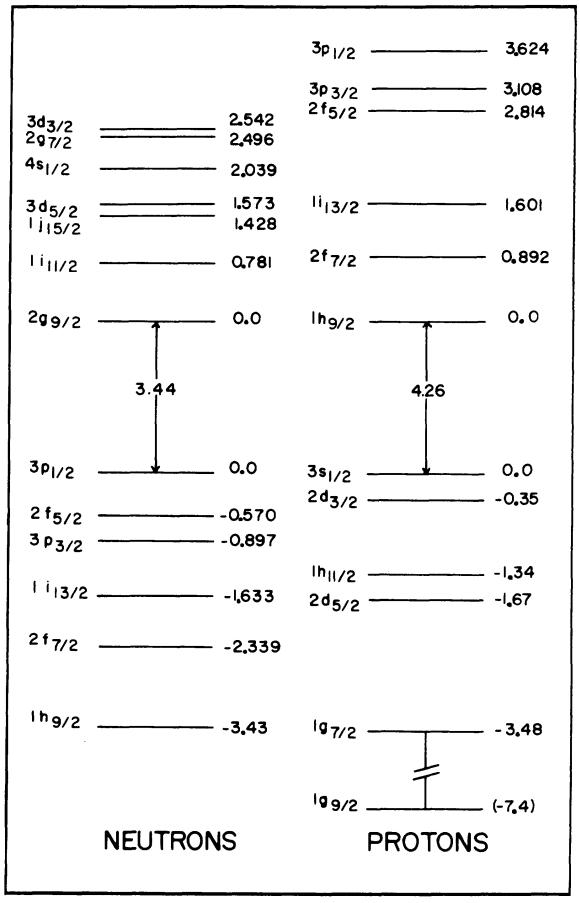

FIG. 1. The experimental single-particle levels in the lead region from Ref. 2. The energies are in MeV.

harmonic-oscillator $N=5$ shell due to the single-particle spin-orbit interaction. This interaction causes the $1i_{13/2}$ orbital from the $N=6$ shell to be included and the $1h_{11/2}$ orbital from the $N=5$ shell to be excluded. The center-of-mass raising and lowering operators have selection rules of $\Delta l=1$ and $\Delta J \leq 1$. But these operators will not connect the $1i_{13/2}$ orbital to any other orbital in the major shell used. So indeed, there are no spurious state problems in the ^{208}Po calculation.

B. Two-hole–two-particle matrix elements

The evaluation of the two-hole–two-particle matrix elements is most conveniently done by using second quantization techniques with the introduction of creation and annihilation operators for the holes and particles.

Let H_i and P_i represent the quantum numbers n_i, l_i, j_i, q_i of the holes and particles, respectively, where q_i represents a charge quantum number to distinguish between neutrons and protons. When H_i or P_i appears in a 3-j, 6-j, etc., coefficient, they will represent j_i only. lH_i and lP_i will be used to represent the l_i for the holes and particles while h_i and p_i will represent the magnetic quantum numbers (z component of j) of the holes and particles.

The ^{206}Pb eigenstates will be a linear combination of the basis states $|H_1H_2J_1M_1\rangle$ and the ^{210}Po eigenstates will be a linear combination of the basis states $|P_1P_2J_2M_2\rangle$. When these basis states are vector coupled together, the two-hole–two-particle correlated basis can be expanded as a linear combination of the two-hole–two-particle states $|H_1H_2J_1, P_1P_2J_2, JM\rangle$ where the coupling scheme is $\vec{l}+\vec{s}=\vec{j}$, $\vec{H}_1+\vec{H}_2=\vec{J}_1$, $\vec{P}_1+\vec{P}_2=\vec{J}_2$, and $\vec{J}_1+\vec{J}_2=\vec{J}$. Antisymmetrization between like particles are implied in these basis states. Some additional notations which will be used below are: $\bar{a}\equiv -a$; $\theta(abc)\equiv(-1)^{a+b+c}$; $\hat{a}\equiv(2a+1)^{1/2}$; $\delta(ab)$ $\equiv$ Kronecker δ function; $\delta(P_1P_2)$ or $\delta(H_1H_2)$ implies $\delta(n_1n_2)\delta(l_1l_2)\delta(j_1j_2)\delta(q_1q_2)$; $|abJ\rangle$ is a vector-coupled two-particle state with $\vec{a}+\vec{b}=\vec{J}$; V is a two-body interaction;

$$\langle abJ|V|cdJ\rangle_{D-X}\equiv\langle abJ|V|cdJ\rangle-\theta(cdJ)\langle abJ|V|dcJ\rangle;$$

$$\begin{pmatrix} a & b & c \\ \alpha & \beta & \gamma \end{pmatrix}\equiv\text{Wigner 3-}j\text{ symbol};$$

$$\begin{Bmatrix} a & b & c \\ d & e & f \end{Bmatrix}\equiv\text{Wigner 6-}j\text{ symbol};$$

$$\begin{Bmatrix} a & b & c \\ d & e & f \\ g & h & i \end{Bmatrix}\equiv\text{Wigner 9-}j\text{ symbol}.$$

The two-hole–two-particle matrix element of V_{hphp} which will be called $\mathfrak{M}$ is given by

$$\begin{aligned}\mathfrak{M}&\equiv\langle H_1H_2J_1, P_1P_2J_2, JM|V_{\text{hphp}}|H_3H_4J_3, P_3P_4J_4, JM\rangle\\&=\frac{\hat{J}_1\hat{J}_2\hat{J}_3\hat{J}_4\theta(H_1H_2H_3H_4P_1P_2P_3P_4J_1J_2J_3J_4)}{\{[1+\delta(H_1H_2)][1+\delta(H_3H_4)][1+\delta(P_1P_2)][1+\delta(P_3P_4)]\}^{1/2}}\\&\times\sum_{\text{all }m\text{'s}}\begin{pmatrix} H_1 & H_2 & J_1 \\ h_1 & h_2 & \bar{M}_1 \end{pmatrix}\begin{pmatrix} P_1 & P_2 & J_2 \\ p_1 & p_2 & \bar{M}_2 \end{pmatrix}\begin{pmatrix} H_3 & H_4 & J_3 \\ h_3 & h_4 & \bar{M}_3 \end{pmatrix}\begin{pmatrix} P_3 & P_4 & J_4 \\ p_3 & p_4 & \bar{M}_4 \end{pmatrix}\begin{pmatrix} J_1 & J_2 & J \\ M_1 & M_2 & \bar{M} \end{pmatrix}\begin{pmatrix} J_3 & J_4 & J \\ M_3 & M_4 & \bar{M} \end{pmatrix}\\&\times\langle H_1h_1, H_2h_2, P_1p_1, P_2p_2|V_{\text{hphp}}|H_3h_3, H_4h_4, P_3p_3, P_4p_4\rangle,\end{aligned}\tag{2}$$

where the sum is over all magnetic quantum numbers. The matrix element on the extreme right-hand side of Eq. (2) can be expressed in terms of creation and annihilation operators which are then put in normal form. This procedure will result in 16 terms for the matrix element $\mathfrak{M}$. The first term which will be called $\mathfrak{M}_1$ is

$$\begin{aligned}\mathfrak{M}_1&=\frac{\hat{J}_1\hat{J}_2\hat{J}_3\hat{J}_4\theta(J_1J_2J_3J_4)\delta(H_2H_4)\delta(P_2P_4)}{\{[1+\delta(H_1H_2)][1+\delta(H_3H_4)][1+\delta(P_1P_2)][1+\delta(P_3P_4)]\}^{1/2}}\sum_{\substack{J'\text{ and}\\ \text{all }m\text{'s}}}\hat{J}'^2\langle P_1H_3J'M'|V|H_1P_3J'M'\rangle_{D-X}\\&\times\theta(H_1h_1H_3h_3)\begin{pmatrix} J_1 & J_2 & J \\ M_1 & M_2 & \bar{M} \end{pmatrix}\begin{pmatrix} J_3 & J_4 & J \\ M_3 & M_4 & \bar{M} \end{pmatrix}\begin{pmatrix} H_1 & H_2 & J_1 \\ h_1 & h_2 & \bar{M}_1 \end{pmatrix}\begin{pmatrix} H_3 & H_2 & J_3 \\ h_3 & h_2 & \bar{M}_3 \end{pmatrix}\\&\times\begin{pmatrix} P_1 & P_2 & J_2' \\ p_1 & p_2 & \bar{M}_2 \end{pmatrix}\begin{pmatrix} P_3 & P_2 & J_4 \\ p_3 & p_2 & \bar{M}_4 \end{pmatrix}\begin{pmatrix} P_1 & H_3 & J' \\ p_1 & \bar{h}_3 & \bar{M}' \end{pmatrix}\begin{pmatrix} H_1 & P_3 & J' \\ \bar{h}_1 & p_3 & \bar{M}' \end{pmatrix}.\end{aligned}\tag{3}$$

The remaining 15 terms can be obtained simply from $\mathfrak{M}_1$ as will be indicated in Eq. (6) below after the sums over the magnetic quantum numbers in Eq. (3) have been done.

Using the identities in the book by Rotenberg *et al.*,[3] the sums over the magnetic quantum numbers in $\mathfrak{M}_1$ can be done. In the Racah algebra below, H_i, h_i, P_i, and p_i will be assumed to be half-integer num-

bers. The successive steps in reducing the matrix element $\mathfrak{M}_1$ are as follows: By Eq. (3.21) of Rotenberg *et al.*[3]

$$\sum_{\substack{p_1,p_2\\p_3,M'}} \begin{pmatrix} P_1 & P_2 & J_2 \\ p_1 & p_2 & \bar{M}_2 \end{pmatrix}\begin{pmatrix} P_3 & P_2 & J_4 \\ p_3 & p_2 & \bar{M}_4 \end{pmatrix}\begin{pmatrix} P_1 & H_3 & J' \\ p_1 & \bar{h}_3 & \bar{M}' \end{pmatrix}\begin{pmatrix} H_1 & P_3 & J' \\ \bar{h}_1 & p_3 & \bar{M}' \end{pmatrix}$$

$$= \sum_{x,m} \theta(H_1P_3J')\hat{x}^2 \begin{pmatrix} J_2 & H_1 & x \\ M_2 & h_1 & m \end{pmatrix}\begin{pmatrix} x & J_4 & H_3 \\ m & M_4 & h_3 \end{pmatrix}\begin{Bmatrix} J_2 & H_1 & x \\ P_2 & P_3 & J_4 \\ P_1 & J' & H_3 \end{Bmatrix};$$

by Eq. (2.20) of Rotenberg *et al.*

$$\sum_{M_1,M_2,h_1} \theta(h_1)\begin{pmatrix} J_1 & J_2 & J \\ M_1 & M_2 & \bar{M} \end{pmatrix}\begin{pmatrix} J_2 & H_1 & x \\ M_2 & h_1 & m \end{pmatrix}\begin{pmatrix} H_1 & H_2 & J_1 \\ h_1 & h_2 & \bar{M}_1 \end{pmatrix} = \theta(H_1H_2xM)\begin{pmatrix} J & x & H_2 \\ \bar{M} & \bar{m} & h_2 \end{pmatrix}\begin{Bmatrix} J & x & H_2 \\ H_1 & J_1 & J_2 \end{Bmatrix};$$

by Eq. (2.18) of Rotenberg *et al.*

$$\sum_{\substack{h_2,h_3,m\\M_3,M_4,M}} \theta(h_3M)\begin{pmatrix} J & x & H_2 \\ \bar{M} & \bar{m} & h_2 \end{pmatrix}\begin{pmatrix} J_3 & J_4 & J \\ M_3 & M_4 & \bar{M} \end{pmatrix}\begin{pmatrix} H_3 & H_2 & J_3 \\ h_3 & h_2 & \bar{M}_3 \end{pmatrix}\begin{pmatrix} x & J_4 & H_3 \\ m & M_4 & h_3 \end{pmatrix} = \theta(H_2H_3x)\begin{Bmatrix} J_3 & J_4 & J \\ x & H_2 & H_3 \end{Bmatrix}.$$

Using the above expressions, one can write $\mathfrak{M}_1$ as

$$\mathfrak{M}_1 = \frac{\hat{J}_1\hat{J}_2\hat{J}_3\hat{J}_4\theta(J_1J_2J_3J_4H_1H_3H_3P_3)\delta(H_2H_4)\delta(P_2P_4)}{\{[1+\delta(H_1H_2)][1+\delta(P_1P_2)][1+\delta(H_3H_4)][1+\delta(P_3P_4)]\}^{1/2}}$$

$$\times \sum_{x,J'} \theta(J'xx)\hat{x}^2\hat{J}'^2 \begin{Bmatrix} J & J_2 & J_1 \\ H_1 & H_2 & x \end{Bmatrix}\begin{Bmatrix} J & J_4 & J_3 \\ H_3 & H_2 & x \end{Bmatrix}\begin{Bmatrix} P_2 & P_3 & J_4 \\ P_1 & J' & H_3 \\ J_2 & H_1 & x \end{Bmatrix}\langle P_1H_3J'M' \mid V \mid H_1P_3J'M'\rangle_{D-X}. \tag{4}$$

The above sum over x can be done using Eq. (4.1) of Rotenberg *et al.*[3] and $\mathfrak{M}_1$ expressed in terms of a 12-j symbol is

$$\mathfrak{M}_1 = \frac{\hat{J}_1\hat{J}_2\hat{J}_3\hat{J}_4\theta(H_3P_3J_1J_3)\delta(H_2H_4)\delta(P_2P_4)}{\{[1+\delta(H_1H_2)][1+\delta(P_1P_2)][1+\delta(H_3H_4)][1+\delta(P_3P_4)]\}^{1/2}} \sum_{J'} \theta(J')\hat{J}'^2 \begin{Bmatrix} P_2 & P_3 & J_4 & J_3 \\ P_1 & J' & H_3 & J_1 \\ J_2 & H_1 & J & H_2 \end{Bmatrix}$$

$$\times \langle P_1H_3J'M' \mid V \mid H_1P_3J'M'\rangle_{D-X}. \tag{5}$$

Equations (4) and (5) are expressions for the first term in the two-hole–two-particle matrix element which holds in general. That is, there is no restriction on the holes and particles being neutrons or protons providing there is the same number of protons and neutrons in each side of the matrix element. The remaining 15 terms in the two-hole–two-particle matrix elements can be easily obtained with Eq. (4) or Eq. (5). Let $\mathfrak{M}_1(H_1 \rightleftarrows H_2)$ represent the matrix element $\mathfrak{M}_1$ of Eq. (4) or Eq. (5) with the quantum numbers implied by H_1 and H_2 interchanged. Similarly $\mathfrak{M}_1(H_1 \rightleftarrows H_2,\ P_1 \rightleftarrows P_2)$ will imply that H_1 and H_2 are interchanged and that P_1 and P_2 are also interchanged. The two-hole–two-particle matrix element $\mathfrak{M}$ is then given by

$$\begin{aligned}
\mathfrak{M} &= \langle H_1H_2J_1, P_1P_2J_2, JM \mid V_{\text{hphp}} \mid H_3H_4J_3, P_3P_4J_4, JM\rangle \\
&= \mathfrak{M}_1 - \theta(H_1H_2J_1)\mathfrak{M}_1(H_1 \rightleftarrows H_2) - \theta(P_1P_2J_2)\mathfrak{M}_1(P_1 \rightleftarrows P_2) - \theta(H_3H_4J_3)\mathfrak{M}_1(H_3 \rightleftarrows H_4) - \theta(P_3P_4J_4)\mathfrak{M}_1(P_3 \rightleftarrows P_4) \\
&\quad + \theta(H_1H_2P_1P_2J_1J_2)\mathfrak{M}_1(H_1 \rightleftarrows H_2,\ P_1 \rightleftarrows P_2) + \theta(H_1H_2H_3H_4J_1J_3)\mathfrak{M}_1(H_1 \rightleftarrows H_2,\ H_3 \rightleftarrows H_4) \\
&\quad + \theta(H_1H_2P_3P_4J_1J_4)\mathfrak{M}_1(H_1 \rightleftarrows H_2,\ P_3 \rightleftarrows P_4) + \theta(P_1P_2H_3H_4J_2J_3)\mathfrak{M}_1(P_1 \rightleftarrows P_2,\ H_3 \rightleftarrows H_4) \\
&\quad + \theta(P_1P_2P_3P_4J_2J_4)\mathfrak{M}_1(P_1 \rightleftarrows P_2,\ P_3 \rightleftarrows P_4) + \theta(H_3H_4P_3P_4J_3J_4)\mathfrak{M}_1(H_3 \rightleftarrows H_4,\ P_3 \rightleftarrows P_4) \\
&\quad - \theta(H_1H_2P_1P_2H_3H_4J_1J_2J_3)\mathfrak{M}_1(H_1 \rightleftarrows H_2,\ P_1 \rightleftarrows P_2,\ H_3 \rightleftarrows H_4) \\
&\quad - \theta(H_1H_2P_1P_2P_3P_4J_1J_2J_4)\mathfrak{M}_1(H_1 \rightleftarrows H_2,\ P_1 \rightleftarrows P_2,\ P_3 \rightleftarrows P_4) \\
&\quad - \theta(H_1H_2H_3H_4P_3P_4J_1J_3J_4)\mathfrak{M}_1(H_1 \rightleftarrows H_2,\ H_3 \rightleftarrows H_4,\ P_3 \rightleftarrows P_4) \\
&\quad - \theta(P_1P_2H_3H_4P_3P_4J_2J_3J_4)\mathfrak{M}_1(P_1 \rightleftarrows P_2,\ H_3 \rightleftarrows H_4,\ P_3 \rightleftarrows P_4) \\
&\quad + \theta(H_1H_2P_1P_2H_3H_4P_3P_4J_1J_2J_3J_4)\mathfrak{M}_1(H_1 \rightleftarrows H_2,\ P_1 \rightleftarrows P_2,\ H_3 \rightleftarrows H_4,\ P_3 \rightleftarrows P_4).
\end{aligned} \tag{6}$$

TABLE I. The nine lowest ^{206}Pb eigenfunctions calculated by Ma and True (Ref. 1). Only the four largest amplitudes and any other amplitudes of magnitude greater than 0.1 are given even though the complete eigenfunctions were used in the ^{208}Po calculation as explained in the text.

J^π, N	E (MeV)	Eigenfunctions						
		$p_{1/2}{}^2$	$f_{5/2}{}^2$	$p_{3/2}{}^2$	$i_{13/2}{}^2$	$f_{7/2}{}^2$		
$0^+, 1$	0.0	0.800	0.400	0.364	−0.187	0.166		
$0^+, 2$	1.106	0.545	−0.745	−0.128	0.307	−0.172		
		$p_{1/2}p_{3/2}$	$f_{5/2}p_{3/2}$					
$1^+, 1$	1.747	1.000	0.000					
		$p_{1/2}f_{5/2}$	$p_{1/2}p_{3/2}$	$f_{5/2}{}^2$	$f_{5/2}p_{3/2}$	$p_{3/2}{}^2$	$p_{3/2}f_{7/2}$	$i_{13/2}{}^2$
$2^+, 1$	0.701	0.708	−0.539	0.268	−0.168	0.205	0.197	···
$2^+, 2$	1.482	0.658	0.731	−0.128	···	−0.118	···	···
$2^+, 3$	1.753	0.166	−0.320	−0.904	···	···	···	0.196
		$p_{1/2}f_{5/2}$	$f_{5/2}p_{3/2}$	$p_{1/2}f_{7/2}$	$f_{5/2}h_{9/2}$			
$3^+, 1$	1.426	1.000	−0.007	0.003	0.010			
		$p_{1/2}f_{7/2}$	$f_{5/2}{}^2$	$f_{5/2}p_{3/2}$	$f_{5/2}f_{7/2}$	$p_{3/2}f_{7/2}$		
$4^+, 1$	1.644	0.275	−0.590	0.717	0.130	−0.147		
$4^+, 2$	2.053	−0.121	−0.794	−0.589	···	0.057		

Equation (6) along with Eq. (4) or (5) can be used to evaluate the two-hole–two-particle matrix element of V_{hphp}. The matrix element $\mathfrak{M}$ will consist in general of less than 16 terms implied by Eq. (6) because of the Kronecker δ functions which appear in each term. However, evaluation of the 12-j coefficients and the sum over J' can be quite time consuming in evaluating the two-hole–two-particle matrix element. This matrix element can be expressed in a different manner so that its numerical evaluation is considerably simplified. The Appendix shows how this matrix element can be rewritten and the final form of $\mathfrak{M}_1$ is given by Eq. (A8).

III. ^{208}Po CALCULATION

A. Correlated basis

The nine lowest eigenfunctions of ^{206}Pb and the five lowest eigenfunctions of ^{210}Po calculated by Ma and True[1] are given in Table I and Table II, respectively. These eigenfunctions represent the results of the first step of a two-step procedure.

As pointed out in Sec. II above, a truncated basis must be chosen in the second step in order that the matrices not be too large. In the results described below, it was found that only the lowest nine levels in ^{206}Pb and the lowest five levels in ^{210}Po need be considered in order to describe the low-lying levels in ^{208}Po. This truncation in the number of levels used from ^{206}Pb and ^{210}Po greatly reduces the size of the Hamiltonian matrix. For example, there are only 20 correlated basis states for $J = 2^+$ instead of about 2500 basis states for a "complete" calculation.

In the ^{210}Po spectrum shown in Fig. 2, there is an energy gap above the first $J = 8^+$ level which indicates that this may be a suitable place to truncate the ^{210}Po states in forming the correlated basis for the low-lying states in ^{208}Po. In ^{206}Pb, there is not such a clear cut energy gap to indicate a suitable place to truncate the ^{206}Pb states. Calculations using the lowest five levels from ^{210}Po and varying numbers of levels from ^{206}Pb

TABLE II. The five lowest ^{210}Po eigenfunctions calculated by Ma and True (Ref. 1). Only the four largest amplitudes and any other amplitudes of magnitude greater than 0.1 are given even though the complete eigenfunctions were used in the ^{208}Po calculations as explained in the text.

J^π, N	E (MeV)	Eigenfunctions			
		$h_{9/2}{}^2$	$f_{7/2}{}^2$	$i_{13/2}{}^2$	$f_{5/2}{}^2$
$0^+, 1$	0.0	0.811	0.357	−0.437	0.145
		$h_{9/2}{}^2$	$h_{9/2}f_{5/2}$	$f_{7/2}{}^2$	$i_{13/2}{}^2$
$2^+, 1$	1.073	0.938	0.076	0.185	−0.264
		$h_{9/2}{}^2$	$h_{9/2}f_{7/2}$	$f_{7/2}{}^2$	$i_{13/2}{}^2$
$4^+, 1$	1.452	0.994	−0.064	0.047	−0.047
		$h_{9/2}{}^2$	$h_{9/2}f_{7/2}$	$f_{7/2}f_{5/2}$	$i_{13/2}{}^2$
$6^+, 1$	1.527	0.998	−0.051	0.020	0.029
		$h_{9/2}{}^2$	$h_{9/2}f_{7/2}$	$i_{13/2}{}^2$	
$8^+, 1$	1.558	0.992	−0.127	−0.026	

showed that the structure of the low-lying levels in ^{208}Po became "stable" when the first nine levels in ^{206}Pb were used.

In Tables I and II only the four largest amplitudes (plus any amplitude whose magnitude is greater than 0.1) is given for each eigenvalue to conserve space. However, the calculations for ^{208}Po described below were done with the complete wave functions containing all the components which had a nonzero amplitude. As pointed out above, the energy eigenvalues and eigenfunctions should give a "good" description of the levels in ^{206}Pb and ^{210}Po in order that the second step of the two-step approach will be meaningful. The eigenstates of Ma and True[1] in Tables I and II do describe ^{206}Pb and ^{210}Po as is indicated by the good agreement between the calculated and experimental energy levels shown in Fig. 2. In addition, these wave functions reproduce fairly well the observed $E2$ and $M1$ transition rates in ^{206}Pb and ^{210}Po as well as the observed spectroscopic distribution in ^{206}Pb and ^{210}Po. (See Ma and True[1] for details.)

The eigenstates of ^{206}Pb and ^{210}Po given in Tables I and II were calculated with an interaction potential

$$V=[V_0e^{-\beta r^2}+\alpha_2 r_1^2 r_2^2 P_2(\cos\theta_{12}) + \alpha_3 r_1^3 r_2^3 P_3(\cos\theta_{12})][P^{\mathrm{SE}}+\eta P^{\mathrm{TE}}], \quad (7)$$

where P^{SE} and P^{TE} are the singlet-even and triplet-even projection operators, respectively. The values for the parameters V_0, β, α_2, α_3, and η are given in Table III. The radial part of the single-particle orbitals is assumed to have a harmonic-oscillator shape with $\nu=0.1842$ fm^{-2}.

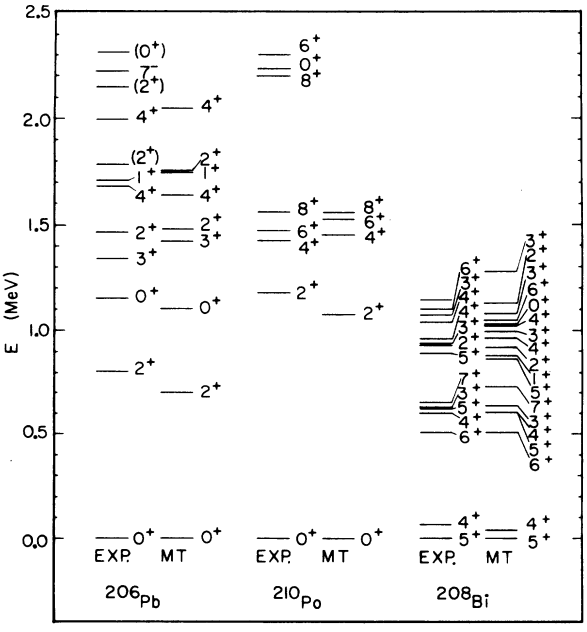

FIG. 2. Comparison of the low-lying experimentally observed levels in ^{206}Pb, ^{210}Po, and ^{208}Bi with those calculated by Ma and True (MT) in Ref. 1.

The eigenfunctions of ^{206}Pb will be written as

$$|(206)J_1N_1\rangle=\sum_{H_1,H_2}A(H_1H_2J_1N_1)|H_1H_2J_1N_1\rangle, \quad (8)$$

where $N_1=1$, 2, etc. denote the first, second, etc. state of angular momentum J_1. Similarly, the states of ^{210}Po will be written as

$$|(210)J_2N_2\rangle=\sum_{P_1,P_2}B(P_1P_2J_2N_2)|P_1P_2J_2N_2\rangle. \quad (9)$$

The states of ^{206}Pb and ^{210}Po are then vector coupled together to form the correlated basis states which will be written as

$$|(206)J_1N_1,(210)J_2N_2,JM\rangle = \sum_{\substack{H_1,H_2\\P_1,P_2}}A(H_1H_2J_1N_1)B(P_1P_2J_2N_2) \times|H_1H_2J_1N_1,\ P_1P_2J_2N_2,\ JM\rangle. \quad (10)$$

These correlated basis states will be used as the basis states in the second step of the two-step calculation. Note that these basis states are already diagonal in $H_{cp}+V_{pppp}$ and $H_{ch}+V_{hhhh}$ with eigenvalues of $E[(206)J_1N_1]$ and $E[(210)J_2N_2]$, respectively.

B. Results for ^{208}Po

The matrix for the Hamiltonian of Eq. (1) with the correlated basis states of Eq. (10) was calculated and diagonalized for each value of J. In calculating the two-hole–two-particle matrix elements, Eq. (6) along with Eq. (A8) was used where the neutron-hole–proton-particle interaction is given by Eq. (7) with the parameters in Table III for ^{208}Bi.

It should be stressed that the neutron-hole–proton-particle interaction parameters were taken from the ^{208}Bi calculation of Ma and True[1] and there are no adjustable parameters. The good

TABLE III. The force parameters V_0, β, α_2, α_3, and η used in the calculations of ^{206}Pb, ^{210}Po, and ^{208}Bi by Ma and True (Ref. 1) and in this paper for ^{208}Po as explained in the text.

	V_0 (MeV)	β (fm^{-2})	α_2 (10^{-4} MeV/fm^4)	α_3 (10^{-4} MeV/fm^6)	η
^{206}Pb	−22.75	0.2922	−5.00	−0.50	1.8
^{210}Po	−22.75	0.2922	−2.50	−1.20	1.8
^{208}Bi	−22.75	0.2922	0.00	−1.95	1.8

agreement between the observed and calculated levels in ^{208}Bi shown in Fig. 2 indicates that the ^{208}Bi force parameters given in Table III do seem to describe fairly well the neutron-hole–proton-particle interaction in the lead region. However, since the truncated model spaces used in the ^{206}Pb, ^{210}Po, and ^{208}Bi are all different from each other and from the model space used in ^{208}Po, the interactions used in the former calculations need not necessarily be the appropriate ones for ^{208}Po. That the interactions are the same implies that ^{208}Pb represents a "good" core in a shell-model sense.

The energy eigenvalues resulting from these calculations are compared with the experimentally observed energy levels[4-9] in Fig. 3. In Fig. 3, Calc. A used the ^{206}Pb and ^{210}Po energy eigenvalues and eigenfunctions calculated by Ma and True.[1] Calc. B, on the other hand, used the experimental energy eigenvalues of ^{206}Pb and ^{210}Po with the eigenfunctions calculated by Ma and True. The main improvement of Calc. B over Calc. A is that the first 2^+ level is in better agreement with the experimentally observed 2^+ level at 0.69 MeV. The higher excited levels are essentially unchanged except in detail. In view of the approximations made in these calculations, the changes of the higher excited levels are not considered significant. For both calculations, the wave functions of ^{208}Po are essentially the same and so only the results of Calc. A will be discussed below.

The spectrum of ^{208}Po has been extensively studied by Treytl, Hyde, and Yamazaki[4] and Yamazaki[5] from the decay of ^{208}At as well as with ^{209}Bi$(p, 2n)$, ^{206}Pb$(\alpha, 2n)$, and ^{208}Pb$(\alpha, 4n)$ reactions. Goldman *et al.*[6] have studied ^{208}Po by observing the internal-conversion electrons following ^{209}Bi$(p, 2n)$ reactions. These and other results are summarized by Lewis in the Nuclear Data Sheets.[7] Recently Bhatia *et al.*[8,9] have identified several new levels in ^{208}Po which were populated in a ^{210}Po(p, t) reaction.

As is seen in Fig. 3, the agreement between the calculated and experimentally observed energy levels is quite good. That is, the first 2^+ state at 0.7 MeV and the group of levels around 1.5 MeV are all well reproduced to within about 100 keV.

Since there is some uncertainty in the experimental data on the group of levels observed around 1.5 MeV, they will be discussed in more detail. The 2^+ levels at 1.26 and 1.54 MeV have recently been observed by Bhatia and co-workers[8,9] and are in good agreement with the two calculated 2^+ levels at 1.21 and 1.65 MeV, respectively. Bhatia and co-workers[8,9] and Treytl, Hyde, and Yamazaki[4] observed a 4^+ level at 1.58 MeV which agrees very well with a calculated 4^+ level at 1.60 MeV. A 4^+ level at 1.35 MeV and a 6^+ level at 1.52 MeV have been observed by Treytl, Hyde, and Yamazaki,[5] and Goldman *et al.*[6] and these levels agree quite well with the calculated 4^+ level at 1.24 MeV and the calculated 6^+ level at 1.55 MeV.

Goldman and co-workers[6] have observed internal-conversion electrons for a transition energy of 1.27 MeV which they believe corresponds to a $E0$ transition to the ground state of ^{208}Po. There is a calculated 0^+ level at 1.38 MeV which could be associated with this observed level.

Lewis[7] reports a level at 1.42 MeV with tentative spin assignments of (2–4). Treytl, Hyde, and Yamazaki[4] assign this level a spin of (3^+) while Goldman *et al.*[6] assign it a spin of 2^+. Lewis[7] indicates that this level decays by an $E2$ transition to the 2_1^+ level at 685 keV. Since there is no experimental evidence that this level decays to the ground state of ^{208}Po, it is possible that this level corresponds to the calculated 0^+ level at 1.38 MeV. If this is the case, then there is no other calculated 0^+ level in this region to explain the 0^+ level at

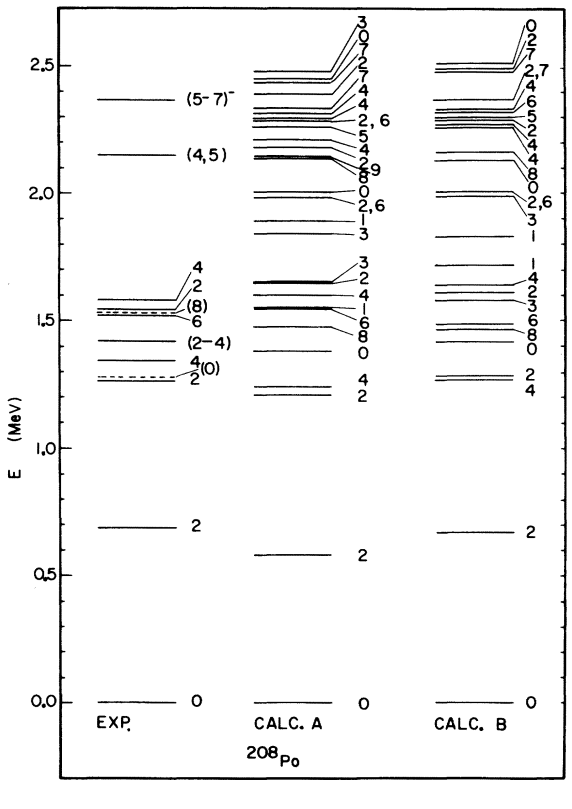

FIG. 3. The experimentally observed levels below 2.5 MeV in ^{208}Po compared with the calculated results. All states have positive parity except for the one experimental level at 2.37 MeV. Calc. A uses the calculated ^{206}Pb and ^{210}Po energies and wave functions of Ma and True (Ref. 1) as input while Calc. B uses the experimental ^{206}Pb and ^{210}Po energies and the calculated wave functions of Ma and True for input as explained in the text.

TABLE IV. Eigenvalues and eigenfunctions of the levels below 2 MeV in ^{208}Po expressed in terms of the correlated basis states, $|(206)J_1N_1, (210)J_2N_2, JM\rangle$, for each spin (the basis configurations are given as J_1N_1, J_2N_2). The energy eigenvalues and their corresponding amplitudes are given if their magnitudes are greater than 0.10. In every case, the four largest nonzero amplitudes are listed even though some may be less than 0.10 in magnitude. With respect to the ^{208}Pb core, $E_{calc.}=5.79$ MeV for the ground state of ^{208}Po while $E_{exp.}=5.84$ MeV.

J^π,N	E (MeV)	Eigenfunctions												
		01,01	02,01	21,21	22,21	23,21	41,41	42,41						
$0^+,1$	0.00	0.935	0.061	−0.349	0.028	···	···	···						
$0^+,2$	1.38	···	−0.948	−0.140	−0.071	0.271	···	···						
$0^+,3$	2.00	−0.310	···	−0.837	···	−0.105	−0.420	0.101						
		11,01	11,21	21,21	22,21	31,41	41,41	42,41						
$1^+,1$	1.55	···	···	0.969	−0.057	···	0.229	−0.051						
$1^+,2$	1.89	0.973	−0.112	···	−0.152	−0.113	···	···						
		01,21	02,21	21,01	22,01	23,01	21,21	22,21	23,21	21,41	31,21	41,21	42,21	41,41
$2^+,1$	0.58	0.513	···	−0.784	···	···	0.304	···	···	···	···	−0.138	···	···
$2^+,2$	1.21	0.724	···	0.496	···	···	···	···	···	−0.419	···	0.199	···	···
$2^+,3$	1.65	···	···	···	0.938	−0.146	···	−0.152	0.117	···	−0.115	···	···	···
$2^+,4$	1.98	···	0.352	···	−0.161	−0.815	···	−0.234	−0.115	···	0.237	···	0.145	0.129
		21,21	22,21	21,41	31,01	31,21	41,21	42,21	41,41					
$3^+,1$	1.65	···	−0.112	···	−0.949	0.219	···	−0.112	···					
$3^+,2$	1.84	0.787	···	−0.507	···	···	−0.249	···	0.201					
		01,41	21,21	21,41	21,61	41,01	42,01	41,21						
$4^+,1$	1.24	0.689	−0.595	0.261	−0.179	−0.223	···	0.109						
$4^+,2$	1.60	−0.505	−0.425	···	0.284	−0.631	0.125	0.229						
		01,61	21,41	21,61	21,81	41,21	41,41	41,61						
$6^+,1$	1.55	0.885	−0.413	···	−0.127	···	···	−0.094						
$6^+,2$	1.99	0.345	0.564	−0.695	···	0.228	−0.107	···						
		01,81	21,61	21,81	41,81									
$8^+,1$	1.48	0.847	−0.067	−0.514	−0.093									

1.27 MeV observed by Goldman and co-workers.[6] The only other "unassigned" calculated levels in this region are a 1^+ level at 1.55 MeV and a 3^+ level at 1.65 MeV. So until more experimental evidence is forthcoming, nothing more can be concluded about these states.

Treytl, Hyde, and Yamazaki[4] and Yamazaki[5] observe that the $6_1^+ \to 4_1^+ \to 2_1^+ \to 0_1^+$ sequence is also fed by a 380-nsec transition although they did not observe the internal-conversion electrons or γ rays associated with the 380-nsec transition. On the basis of this evidence, they conclude that an 8^+ level located about 10 keV above the 6_1^+ level is decaying by an $E2$ transition to the 6_1^+ level. An 8^+ level is calculated at 1.48 MeV and could be a candidate for an unobserved 8^+ level at 1.53 MeV. However, more experimental information is needed before definite statements can be made.

The wave functions of the low-lying states of ^{208}Po expressed in terms of the correlated basis states $|(206)J_1N_1, (210)J_2N_2, JM\rangle$ are given in Table IV. Although some configuration mixing takes place, it is seen in Table IV that many of the low-lying states in ^{208}Po still have a single dominant component of over 60%. This lack of configuration mixing verifies that the correlated basis space can be severely truncated and still give a very good description of the ^{208}Po levels. Note also that the strong neutron-hole correlations of ^{206}Pb and the strong proton-particle correlations of ^{210}Po have been retained. If this was not the case, one would have been forced to use a much larger correlated basis space to describe the low-lying ^{208}Po levels.

The wave functions of ^{208}Po can also be expressed in terms of the two-hole–two-particle basis $|H_1H_2J_1, P_1P_2J_2, JM\rangle$ by multiplying together the corresponding amplitudes in Tables I, II, and IV. This has been done for the low-lying levels of ^{208}Po and the major components of the wave functions in terms of the two-hole–two-particle basis are given in Table V. It is seen from Table V that, in general, the configuration mixing appearing in

TABLE V. The eigenfunctions of the low-lying levels of ^{208}Po expressed in terms of a two-neutron-hole–two-proton-particle basis. The only basis states listed below are those which have an amplitude whose magnitude is greater than 0.3 and are denoted by $|\bar{H}_1\bar{H}_2J_1, P_1P_2J_2, J\rangle$.

J^π, N	E (MeV)	Eigenfunctions
$0^+, 1$	0.00	$0.607\|\bar{p}_{1/2}{}^20, h_{9/2}{}^20, 0\rangle + 0.303\|\bar{f}_{5/2}{}^20, h_{9/2}{}^20, 0\rangle - 0.327\|\bar{p}_{1/2}{}^20, i_{13/2}{}^20, 0\rangle$
$0^+, 2$	1.38	$-0.419\|\bar{p}_{1/2}{}^20, h_{9/2}{}^20, 0\rangle + 0.573\|\bar{f}_{5/2}{}^20, h_{9/2}{}^20, 0\rangle - 0.309\|\bar{f}_{5/2}{}^20, i_{13/2}{}^20, 0\rangle$
$0^+, 3$	2.00	$-0.556\|\bar{p}_{1/2}\bar{f}_{5/2}2, h_{9/2}{}^22, 0\rangle + 0.423\|\bar{p}_{1/2}\bar{p}_{3/2}2, h_{9/2}{}^22, 0\rangle$
$1^+, 1$	1.55	$0.644\|\bar{p}_{1/2}\bar{f}_{5/2}2, h_{9/2}{}^22, 1\rangle - 0.490\|\bar{p}_{1/2}\bar{p}_{3/2}2, h_{9/2}{}^22, 1\rangle$
$1^+, 2$	1.89	$0.789\|\bar{p}_{1/2}\bar{p}_{3/2}1, h_{9/2}{}^20, 1\rangle + 0.347\|\bar{p}_{1/2}\bar{p}_{3/2}1, f_{7/2}{}^20, 1\rangle - 0.425\|\bar{p}_{1/2}\bar{p}_{3/2}1, i_{13/2}{}^20, 1\rangle$
$2^+, 1$	0.58	$0.385\|\bar{p}_{1/2}{}^20, h_{9/2}{}^22, 2\rangle - 0.450\|\bar{p}_{1/2}\bar{f}_{5/2}2, h_{9/2}{}^20, 2\rangle + 0.343\|\bar{p}_{1/2}\bar{p}_{3/2}2, h_{9/2}{}^20, 2\rangle$
$2^+, 2$	1.21	$0.543\|\bar{p}_{1/2}{}^20, h_{9/2}{}^22, 2\rangle$
$2^+, 3$	1.65	$0.501\|\bar{p}_{1/2}\bar{f}_{5/2}2, h_{9/2}{}^20, 2\rangle + 0.556\|\bar{p}_{1/2}\bar{p}_{3/2}2, h_{9/2}{}^20, 2\rangle - 0.300\|\bar{p}_{1/2}\bar{p}_{3/2}2, i_{13/2}{}^20, 2\rangle$
$2^+, 4$	1.98	$0.598\|\bar{f}_{5/2}{}^22, h_{9/2}{}^20, 2\rangle - 0.322\|\bar{f}_{5/2}{}^22, i_{13/2}{}^20, 2\rangle$
$3^+, 1$	1.65	$-0.770\|\bar{p}_{1/2}\bar{f}_{5/2}3, h_{9/2}{}^20, 3\rangle - 0.339\|\bar{p}_{1/2}\bar{f}_{5/2}3, f_{7/2}{}^20, 3\rangle + 0.415\|\bar{p}_{1/2}\bar{f}_{5/2}3, i_{13/2}{}^20, 3\rangle$
$3^+, 2$	1.84	$0.523\|\bar{p}_{1/2}\bar{f}_{5/2}2, h_{9/2}{}^22, 3\rangle - 0.398\|\bar{p}_{1/2}\bar{p}_{3/2}2, h_{9/2}{}^22, 3\rangle - 0.357\|\bar{p}_{1/2}\bar{f}_{5/2}2, h_{9/2}{}^24, 3\rangle$
$4^+, 1$	1.24	$0.548\|\bar{p}_{1/2}{}^20, h_{9/2}{}^24, 4\rangle - 0.395\|\bar{p}_{1/2}\bar{f}_{5/2}2, h_{9/2}{}^22, 4\rangle + 0.301\|\bar{p}_{1/2}\bar{p}_{3/2}2, h_{9/2}{}^22, 4\rangle$
$4^+, 2$	1.60	$-0.402\|\bar{p}_{1/2}{}^20, h_{9/2}{}^24, 4\rangle + 0.302\|\bar{f}_{5/2}{}^24, h_{9/2}{}^20, 4\rangle - 0.367\|\bar{f}_{5/2}\bar{p}_{3/2}4, h_{9/2}{}^20, 4\rangle$
$6^+, 1$	1.55	$0.707\|\bar{p}_{1/2}{}^20, h_{9/2}{}^26, 6\rangle + 0.353\|\bar{f}_{5/2}{}^20, h_{9/2}{}^26, 6\rangle + 0.321\|\bar{p}_{3/2}{}^20, h_{9/2}{}^26, 6\rangle$
$6^+, 2$	1.99	$0.397\|\bar{p}_{1/2}\bar{f}_{5/2}2, h_{9/2}{}^24, 6\rangle - 0.302\|\bar{p}_{1/2}\bar{p}_{3/2}2, h_{9/2}{}^24, 6\rangle - 0.491\|\bar{p}_{1/2}\bar{f}_{5/2}2, h_{9/2}{}^26, 6\rangle + 0.374\|\bar{p}_{1/2}\bar{p}_{3/2}2, h_{9/2}{}^26, 6\rangle$
$8^+, 1$	1.48	$0.672\|\bar{p}_{1/2}{}^20, h_{9/2}{}^28, 8\rangle + 0.336\|\bar{f}_{5/2}{}^20, h_{9/2}{}^28, 8\rangle + 0.306\|\bar{p}_{3/2}{}^20, h_{9/2}{}^28, 8\rangle - 0.361\|\bar{p}_{1/2}\bar{f}_{5/2}2, h_{9/2}{}^28, 8\rangle$

these wave functions is now much larger and that there is no dominant configuration when one considers a two-hole–two-particle basis. Consequently any calculation of ^{208}Po with a two-hole–two-particle basis would be in doubt unless the complete two-hole–two-particle basis was used.

Using the ^{208}Po wave functions in Table IV, the $B(E2)$ transition rates for the $8_1^+ \to 6_1^+ \to 4_1^+ \to 0_1^+$ sequence have been calculated and are given in Table VI. The effective charges were 0.87 e for the neutrons and 1.50 e for the protons and are the values used by Ma and True[1] in ^{206}Pb and ^{210}Po, respectively. However, the effective charges are expected to depend more sensitively on the model space used than does the effective interaction, and it is not clear that the effective charges used in ^{206}Pb and ^{210}Po are necessarily the appropriate ones to use in ^{208}Po.

If we assume that the $8_1^+ \to 6_1^+$ transition has a half-life of 380 nsec as suggested by Yamazaki,[5] the calculated $B(E2)$ value of 85 e^2 fm^4 from Table VI indicates a transition energy of less than 15 keV. (See Sec. IV of Yamazaki[5] for details.) This very low value for the transition energy is probably the reason why this transition was not observed by Yamazaki[5] or Treytl, Hyde, and Yamazaki.[4] The calculated $B(E2)$ value of 531 e^2 fm^4 for the $6_1^+ \to 4_1^+$ transition is considered to be in reasonably good agreement with the experimental value of 450 e^2 fm^4 as determined by Treytl, Hyde, and Yamazaki.[4] This calculated $B(E2)$ value of 531 e^2 fm^4 and the experimental value of 450 e^2 fm^4 are to be compared with an observed $B(E2)$ value of 245 e^2 fm^4 for the $6_1^+ \to 4_1^+$ transition in ^{210}Po indicating an enhancement in the ^{208}Po case.

In addition to the eigenvalues and eigenfunctions given in Table IV for the calculated levels below 2 MeV, the lowest calculated levels for $J = 9^+$, 10^+, 11^+, and 12^+ are at 2.15, 2.53, 3.14, and 3.64 MeV, respectively.

C. "Weak-coupling" model for ^{210}Po

It is possible to obtain a fairly good indication of what the low-lying spectrum of ^{208}Po will look like by just vector coupling together the observed low-lying states of ^{206}Pb and ^{210}Po and neglecting the neutron-hole–proton-particle interaction ($V_{\text{hphp}} = 0$). This weak-coupling approach is com-

TABLE VI. The calculated $B(E2)$'s in ^{208}Po for the $8_1^+ \to 6_1^+ \to 4_1^+ \to 2_1^+ \to 0_1^+$ sequence.

$J^\pi_i \to J^\pi_f$	$8_1^+ \to 6_1^+$	$6_1^+ \to 4_1^+$	$4_1^+ \to 2_1^+$	$2_1^+ \to 0_1^+$
$B(E2)$ (e^2 fm^4)	85	531	733	649

pared in Fig. 4 to the experimental ^{208}Po spectrum and the calculated ^{208}Po spectrum of this paper which uses as input the experimental energies of ^{206}Pb and ^{210}Po (Calc. B of Sec. III B).

Figure 4 indicates that the weak-coupling calculation does reasonably well in describing the low-lying levels of ^{208}Po. However, when the neutron-hole–proton-particle interaction is included, considerable energy shifts and reordering of the levels above 1 MeV take place. Figure 4 indicates that the more detailed microscopic calculation appears to give better agreement with the experimentally observed levels than the weak-coupling picture does.

As indicated in Table IV, the eigenfunctions in ^{208}Po contain for the most part relatively little configuration mixing of the correlated basis states. Consequently, it would be difficult to distinguish experimentally between the weak-coupling case and the more complete microscopic calculation done in this paper. The two lowest 2^+ states and the two lowest 4^+ states are exceptions to the above rule in that their largest component is less than 65% of that predicted by the weak-coupling picture. Consequently these three states could be used as an experimental test of the calculated wave functions.

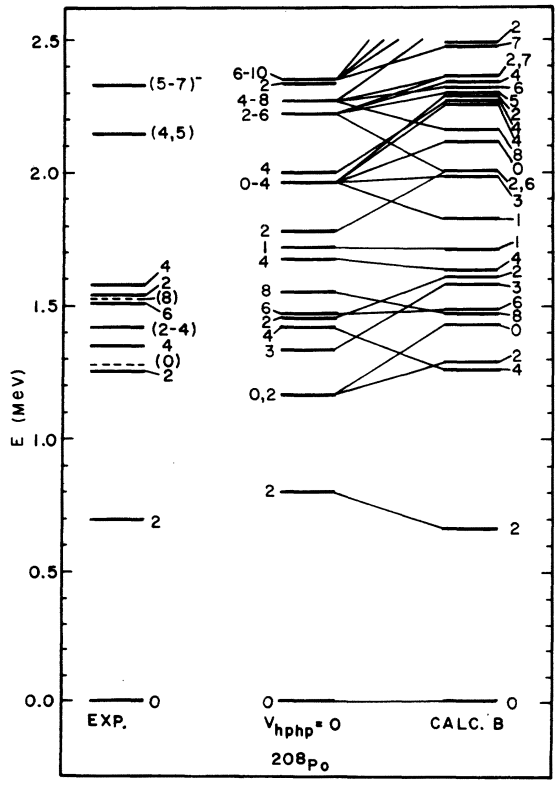

FIG. 4. Comparison between the ^{208}Po experimentally observed levels, the levels in the weak-coupling approximation, and the levels from the more detailed microscopic calculation (Calc. B). All states have positive parity except for the one experimental level at 2.37 MeV.

Another experimental fact which favors the more detailed microscopic calculation over the weak-coupling picture is the observed $B(E2)$ value of 450 e^2 fm^4 for the $6_1^+ \rightarrow 4_1^+$ transition in ^{208}Po. The weak-coupling picture predicts that this $B(E2)$ should be the same as the corresponding $6_1^+ \rightarrow 4_1^+$ $E2$ transition in ^{210}Po which has a $B(E2)$ value of 245 e^2 fm^4. The calculated $B(E2)$ value of 531 e^2 fm^4 is in better agreement with the experimental value.

Lastly, the experimental binding energy of ^{208}Po with respect to the ^{208}Pb ground state is 5.84 MeV. The weak-coupling picture predicts a binding energy of 5.33 MeV while the calculation described in this paper gives a binding energy of 5.79 MeV which is closer to the observed value.

D. Remarks on isospin violation

The Hamiltonian used in this paper violates isospin conservation in two ways as discussed below.

Even though the neutron holes and proton particles are restricted to the same major shell, the single-particle spacings used for the neutron holes in the ^{206}Pb calculation are different from the single-particle spacings used for the proton particles in the ^{210}Po calculation as can be seen in Fig. 1. These single-particle spacings are experimental[2] and to date, there are no theoretical calculations, Hartree-Fock or otherwise, which can explain why these single-particle spectra differ. Presumably this difference can be associated with the fact that the neutron orbitals describe neutron holes in the ^{208}Pb core while the proton orbitals describe proton particles outside the ^{208}Pb core. The lack of an alternative prescription for the neutron-hole and proton-particle orbitals, and the reasonably good fits obtained by Ma and True[1] to the observed levels of ^{206}Pb and ^{210}Po indicate that one is justified in using these non-isospin-conserving single-particle spacings.

Furthermore, it is expected that this isospin-violating Hamiltonian will give about the same re-

TABLE VII. Comparison between the squared amplitudes of the calculated analog state in ^{208}Bi and those of a pure analog state. $T = 22$ is the isospin of the ^{208}Pb ground state.

$\bar{j}_n j_p$	$\bar{h}_{9/2}h_{9/2}$	$\bar{f}_{7/2}f_{7/2}$	$\bar{i}_{13/2}i_{13/2}$	$\bar{f}_{5/2}f_{5/2}$	$\bar{p}_{3/2}p_{3/2}$	$\bar{p}_{1/2}p_{1/2}$
^{208}Bi	0.24	0.19	0.26	0.15	0.12	0.05
$\frac{2j+1}{2T}$	0.23	0.18	0.32	0.14	0.09	0.05

sults as an isospin-conserving Hamiltonian. The isobaric analog state to the ^{208}Pb ground state, a highly excited 0^+ state in ^{208}Bi, has been calculated by True, Ma, and Pinkston[10] and their results are compared to a pure analog state in Table VII. The small differences in Table VII between the square amplitudes of the ^{208}Bi configurations and those for a pure analog state indicate that the isospin-violating effects are small.

The second place that the Hamiltonian used in this paper violates isospin conservation is that the parameters α_2 and α_3 in the residual interaction given by Eq. (7) take on different values for ^{206}Pb, ^{210}Po, and ^{208}Bi. As discussed by Ma and True[1] (Sec. II) a residual force given by Eq. (7) with $\alpha_2 = \alpha_3 = 0$, gives a fairly good fit to the nuclei in the lead region providing one does not mind one or two levels on the average per nucleus deviating from the observed levels by about 200 keV. The isospin-violating nonidentical values α_2 and α_3 for V_{pppp}, V_{hhhh}, and V_{hphp} are not expected to make any large quantitative changes in a ^{208}Po calculation as compared to a calculation where identical values or even zero are used for α_2 and α_3 in V_{pppp}, V_{hhhh}, and V_{hphp} since the levels used from ^{206}Pb and ^{210}Po are not very sensitive to variations in these parameters.

IV. CONCLUSIONS

It is seen that a two-step shell-model calculation gives a fairly good energy fit to the observed low-lying energy levels of ^{208}Po. However, more experimental information is needed on ^{208}Po before a more detailed comparison between the calculated results and the experimental results can be made. It should be stressed that there were no adjustable parameters in this calculation as the basis wave functions, zero-order energies, and the effective interactions were all taken directly from the previous work of Ma and True[1] on ^{206}Pb, ^{210}Po, and ^{208}Bi.

This calculation on the energy levels of ^{208}Po indicate that a two-step shell-model calculation is a valid approach which works whereas a conventional one-step shell-model calculation is essentially impossible because of the very large matrices which must be diagonalized. The two-step shell model appears to have a wide range of applicability and could, in principle, be applied to many nuclei—even those away from a doubly magic nucleus where conventional one-step shell-model calculations are essentially impossible to do. The authors would like to note that Glendenning and Harada[11] have previously done a two-step shell-model calculation for ^{212}Po where they used truncated single-particle orbital spaces to calculate the ^{210}Pb and ^{210}Po eigenfunctions instead of using all the orbitals in the appropriate major shell.

The authors would like to thank Professor P. D. Barnes for sending us his recent experimental results prior to publication.

APPENDIX

Equations (5) and (6) enable one to evaluate the two-hole–two-particle matrix element

$$\mathfrak{M} = \langle H_1 H_2 J_1, P_1 P_2 J_2, JM \,|\, V_{\text{hphp}} | H_3 H_4 J_3, P_3 P_4 J_4, JM \rangle .$$

However, if these expressions are used to actually calculate the matrix element, the sum over J' and the evaluation of the 12-j coefficients can be quite time consuming. The expression for $\mathfrak{M}$ can be considerably "simplified" for computational purposes as will be shown below. For this purpose, consider a central force

$$V = V(r)(W + MP^r + BP^\sigma + HP^r P^\sigma), \tag{A1}$$

where P^r and P^σ are the space-exchange and spin-exchange operators, respectively.

In Eq. (5), the 12-j symbol will be replaced using Eq. (4.1) of Rotenberg *et al.*,[3] viz.

$$\begin{Bmatrix} P_2 & P_3 & J_4 & J_3 \\ P_1 & J' & H_3 & J_1 \\ J_2 & H_1 & J_2 & H_2 \end{Bmatrix} = \sum_x \theta(H_1 H_2 H_3 P_1 P_2 P_3 J_1 J_2 J_3 J_4 J' J \bar{x}) \hat{x}^2 \begin{Bmatrix} P_3 & P_1 & x \\ J_2 & J_4 & P_2 \end{Bmatrix} \begin{Bmatrix} J_2 & J_4 & x \\ J_3 & J_1 & J \end{Bmatrix} \begin{Bmatrix} J_3 & J_1 & x \\ H_1 & H_3 & H_2 \end{Bmatrix} \begin{Bmatrix} H_1 & H_3 & x \\ P_1 & P_3 & J' \end{Bmatrix}.$$

Next the jj matrix element in Eq. (5) is transformed to the LS coupling scheme yielding a LS matrix element of

$$\langle lP_1 lH_3 LS \,|\, V \,|\, lH_1 lP_3 LS \rangle_{D-X} .$$

In the general case, the particles and holes can be either neutrons or protons and one has the general rela-

tion

$$\begin{aligned}\langle l_1 l_2 LS|\, V\,|\, l_3 l_4 LS\rangle_{D-X} &= \langle l_1 l_2 LS|\, V(r)(W + MP^r + BP^\sigma + HP^r P^\sigma)\,|\, l_3 l_4 LS\rangle_{D-X} \\ &= [W\delta(q_1 q_3)\delta(q_2 q_4) - H\delta(q_1 q_4)\delta(q_2 q_3)]\langle l_1 l_2 L|\, V(r)\,|\, l_3 l_4 L\rangle \\ &\quad + \theta(S)[M\delta(q_1 q_4)\delta(q_2 q_3) - B\delta(q_1 q_3)\delta(q_2 q_4)]\langle l_1 l_2 L|\, V(r)\,|\, l_3 l_4 L\rangle \\ &\quad + \theta(l_3 l_4 L)[M\delta(q_1 q_3)\delta(q_2 q_4) - B\delta(q_1 q_4)\delta(q_2 q_3)]\langle l_1 l_2 L|\, V(r)\,|\, l_4 l_3 L\rangle \\ &\quad + \theta(l_3 l_4 LS)[W\delta(q_1 q_4)\delta(q_2 q_3) - H\delta(q_1 q_3)\delta(q_2 q_4)]\langle l_1 l_2 L|\, V(r)\,|\, l_4 l_3 L\rangle\,, \end{aligned} \tag{A2}$$

where q_i is the charge quantum number associated with the particle having the quantum number l_i.

For the special case of ^{208}Po, where the holes are neutrons and the particles are protons, this LS matrix element reduces to

$$\begin{aligned}\langle lP_1 lH_3 LS|\, V\,|\, lH_1 lP_3 LS\rangle_{D-X} &= -H\langle lP_1 lH_3 L|\, V(r)\,|\, lH_1 lP_3 L\rangle + \theta(S)M\langle lP_1 lH_3 L|\, V(r)\,|\, lH_1 lP_3 L\rangle \\ &\quad - \theta(lH_1 lP_3 L)B\langle lP_1 lH_3 L|\, V(r)\,|\, lP_3 lH_1 L\rangle + \theta(lH_1 lP_3 LS)W\langle lP_1 lH_3 L|\, V(r)\,|\, lP_3 lH_1 L\rangle\,. \end{aligned} \tag{A3}$$

The LS matrix element $\langle l_1 l_2 L|\, V(r)\,|\, l_3 l_4 L\rangle$ can be expanded in the conventional way, viz.

$$\langle l_1 l_2 L|\, V(r)\,|\, l_3 l_4 L\rangle = \theta(l_2 l_3 L)\sum_k R^k(l_1 l_2 l_3 l_4)\langle l_1\|C^k\|l_3\rangle\langle l_2\|C^k\|l_4\rangle \begin{Bmatrix} l_1 & l_2 & L \\ l_4 & l_3 & k \end{Bmatrix} \tag{A4}$$

which defines the conventional Slater integral $R^k(l_1 l_2 l_3 l_4)$ while $\langle l_1\|C^k\|l_3\rangle$ is the reduced matrix element defined by Racah.[3,12] That is,

$$\langle l_1 m_1|\, C_q^k\,|\, l_2 m_2\rangle = \theta(l_1 \bar{m}_1)\begin{pmatrix} l_1 & k & l_2 \\ \bar{m}_1 & q & m_2 \end{pmatrix}\langle l_1\|C^k\|l_2\rangle\,,$$

where

$$C_q^k \equiv \left(\frac{4\pi}{2k+1}\right)^{1/2} Y_q^k(\theta,\phi)\,.$$

For conciseness in notation in reducing the matrix element $\mathfrak{M}_1$, the following notation will be used:

$$\alpha \equiv \frac{\delta(H_2 H_4)\delta(P_2 P_4)\hat{J}_1\hat{J}_2\hat{J}_3\hat{J}_4\hat{H}_1\hat{P}_1\hat{H}_3\hat{P}_3}{\{[1+\delta(H_1 H_2)][1+\delta(H_3 H_4)][1+\delta(P_1 P_2)][1+\delta(P_3 P_4)]\}^{1/2}}\,, \tag{A5a}$$

$$\beta(x) \equiv \begin{Bmatrix} P_3 & P_1 & x \\ J_2 & J_4 & P_2 \end{Bmatrix}\begin{Bmatrix} J_3 & J_4 & x \\ J_3 & J_1 & J \end{Bmatrix}\begin{Bmatrix} J_3 & J_1 & x \\ H_1 & H_3 & H_2 \end{Bmatrix}, \tag{A5b}$$

$$\gamma_D(k) \equiv R^k(P_1 H_3 H_1 P_3)\langle lP_1\|C^k\|lH_1\rangle\langle lH_3\|C^k\|lP_3\rangle\,, \tag{A5c}$$

$$\gamma_X(k) \equiv R^k(P_1 H_3 P_3 H_1)\langle lP_1\|C^k\|lP_3\rangle\langle lH_3\|C^k\|lH_1\rangle\,, \tag{A5d}$$

$$D_1 \equiv W\delta(q_1 q_3)\delta(q_2 q_4) - H\delta(q_1 q_4)\delta(q_2 q_3)\,, \tag{A5e}$$

$$D_2 \equiv M\delta(q_1 q_4)\delta(q_2 q_3) - B\delta(q_1 q_3)\delta(q_2 q_4)\,, \tag{A5f}$$

$$X_1 \equiv M\delta(q_1 q_3)\delta(q_2 q_4) - B\delta(q_1 q_4)\delta(q_2 q_3)\,, \tag{A5g}$$

$$X_2 \equiv W\delta(q_1 q_4)\delta(q_2 q_3) - H\delta(q_1 q_3)\delta(q_2 q_4)\,. \tag{A5h}$$

With the notation indicated in Eq. (A5) above, the $\mathfrak{M}_1$ matrix element can now be written as

$$\mathfrak{M}_1 = \alpha \sum_{\substack{x,k \\ L,S,J'}} \beta(x)\hat{J}'^2\hat{S}^2\hat{L}^2\hat{x}^2\theta(JJ_2J_4LH_1H_2P_1P_2lH_1lH_3x) \begin{Bmatrix} H_1 & H_3 & x \\ P_1 & P_3 & J' \end{Bmatrix} \begin{Bmatrix} \frac{1}{2} & \frac{1}{2} & S \\ P_1 & H_3 & J' \\ lP_1 & lH_3 & L \end{Bmatrix} \begin{Bmatrix} \frac{1}{2} & \frac{1}{2} & S \\ H_1 & P_3 & J' \\ lH_1 & lP_3 & L \end{Bmatrix}$$

$$\times \left([D_1\gamma_D(k) + \theta(S)D_2\gamma_D(k)] \begin{Bmatrix} lP_1 & lH_3 & L \\ lP_3 & lH_1 & k \end{Bmatrix} + [\theta(L)X_1\gamma_X(k) + \theta(LS)X_2\gamma_X(k)] \begin{Bmatrix} lP_1 & lH_3 & L \\ lH_1 & lP_3 & k \end{Bmatrix} \right). \quad \text{(A6)}$$

$\mathfrak{M}_1$ in Eq. (A6) is seen to consist of sums over four terms and will be written as

$$\mathfrak{M}_1 = \mathfrak{M}_{11} + \mathfrak{M}_{12} + \mathfrak{M}_{13} + \mathfrak{M}_{14},$$

where $\mathfrak{M}_{11}$ refers to the term with $D_1\gamma_D(k)$, $\mathfrak{M}_{12}$ to the term with $\theta(S)D_2\gamma_D(k)$, $\mathfrak{M}_{13}$ to the term with $\theta(L)X_1\gamma_X(k)$, and $\mathfrak{M}_{14}$ to the term with $\theta(LS)X_2\gamma_X(k)$.

The sums over L, S, and J' in $\mathfrak{M}_{11}$ can now be done in the following manner. Using Eq. (3) of Talman and True,[13] the sum over L gives

$$\sum_L \theta(L)\hat{L}^2 \begin{Bmatrix} lP_1 & lH_3 & L \\ lP_3 & lH_1 & k \end{Bmatrix} \begin{Bmatrix} \frac{1}{2} & \frac{1}{2} & S \\ P_1 & H_3 & J' \\ lP_1 & lH_3 & L \end{Bmatrix} \begin{Bmatrix} \frac{1}{2} & \frac{1}{2} & S \\ H_1 & P_3 & J' \\ lH_1 & lP_3 & L \end{Bmatrix}$$

$$= -\sum_{A,C} \theta(ACSJ'kH_1H_3lP_1lP_3)\hat{A}^2\hat{C}^2 \begin{Bmatrix} \frac{1}{2} & \frac{1}{2} & S \\ \frac{1}{2} & \frac{1}{2} & A \end{Bmatrix} \begin{Bmatrix} P_1 & H_3 & J' \\ P_3 & H_1 & C \end{Bmatrix} \begin{Bmatrix} \frac{1}{2} & \frac{1}{2} & A \\ P_1 & H_1 & C \\ lP_1 & lH_1 & k \end{Bmatrix} \begin{Bmatrix} \frac{1}{2} & \frac{1}{2} & A \\ H_3 & P_3 & C \\ lH_3 & lP_3 & k \end{Bmatrix}.$$

Using Eq. (2.10) of Rotenberg *et al.*[3]

$$\sum_S \theta(S)\hat{S}^2 \begin{Bmatrix} \frac{1}{2} & \frac{1}{2} & S \\ \frac{1}{2} & \frac{1}{2} & A \end{Bmatrix} = -2\delta_{A0}$$

which implies that $C = k$ only (see the 9-j coefficients above) and so the sums over A and C are eliminated. Using Eq. (2.7) of Rotenberg *et al.*, the sum over J' gives

$$\sum_{J'} \theta(J'kx)\hat{J}'^2 \begin{Bmatrix} H_1 & H_3 & x \\ P_1 & P_3 & J' \end{Bmatrix} \begin{Bmatrix} P_1 & H_3 & J' \\ P_3 & H_1 & k \end{Bmatrix} = \begin{Bmatrix} H_1 & H_3 & x \\ P_3 & P_1 & k \end{Bmatrix}.$$

As $A = 0$ and $C = k$, the two 9-j coefficients above can be reduced to two 6-j coefficients. Consequently the first term in Eq. (A6) can be written as

$$\mathfrak{M}_{11} = \alpha D_1 \sum_{x,k} \beta(x)\gamma_D(k)\hat{x}^2\theta(JJ_2J_4H_1H_2H_3P_1P_2P_3lH_1lP_3k) \begin{Bmatrix} H_1 & H_2 & x \\ P_3 & P_1 & k \end{Bmatrix} \begin{Bmatrix} P_1 & H_1 & k \\ lH_1 & lP_1 & \frac{1}{2} \end{Bmatrix} \begin{Bmatrix} H_3 & P_3 & k \\ lP_3 & lH_3 & \frac{1}{2} \end{Bmatrix}. \quad \text{(A7)}$$

At this point it appears that the single sum over J' in Eq. (5) has been replaced by a double sum over x and k in Eq. (A7). However, Eq. (A7) is really much simpler because the 12-j symbol in Eq. (5) requires a sum over x to evaluate it. In addition, the matrix element in Eq. (5) has to be transformed to the LS coupling scheme and then expanded in terms of Slater integrals, reduced matrix elements, etc. So to evaluate Eq. (5), one would have to sum over J', L, S, x, and k and clearly Eq. (A7) is a great simplification.

$\mathfrak{M}_{12}$, $\mathfrak{M}_{13}$, and $\mathfrak{M}_{14}$ can also be reduced using similar methods as were used in the reduction of $\mathfrak{M}_{11}$ above.

The matrix element $\mathfrak{M}_1$ can then be written as

$$\begin{aligned}\mathfrak{M}_1 &= \mathfrak{M}_{11}+\mathfrak{M}_{12}+\mathfrak{M}_{13}+\mathfrak{M}_{14}\\ &= \alpha\theta(JJ_2J_4H_1H_2H_3P_1P_2P_3lH_1lP_3)\\ &\times\Bigg[\sum_{k,x} D_1\beta(x)\gamma_D(k)\hat{x}^2\theta(k)\begin{Bmatrix}H_1 & H_3 & x\\ P_3 & P_1 & k\end{Bmatrix}\begin{Bmatrix}P_1 & H_1 & k\\ lH_1 & lP_1 & \frac{1}{2}\end{Bmatrix}\begin{Bmatrix}H_3 & P_3 & k\\ lP_3 & lH_3 & \frac{1}{2}\end{Bmatrix}\\ &+\sum_{k,x} D_2\beta(x)\gamma_D(k)\hat{x}^2\theta(k)\begin{Bmatrix}lP_1 & lH_1 & k\\ lH_3 & lP_3 & x\end{Bmatrix}\begin{Bmatrix}lH_1 & lH_3 & x\\ H_3 & H_1 & \frac{1}{2}\end{Bmatrix}\begin{Bmatrix}lP_3 & lP_1 & x\\ P_1 & P_3 & \frac{1}{2}\end{Bmatrix}\\ &+\sum_{k,x,q} X_1\beta(x)\gamma_X(k)\hat{x}^2\hat{q}^2\theta(k)\begin{Bmatrix}H_1 & H_3 & x\\ P_3 & P_1 & q\end{Bmatrix}\begin{Bmatrix}lP_1 & lP_3 & k\\ lH_3 & lH_1 & q\end{Bmatrix}\begin{Bmatrix}lP_1 & lH_1 & q\\ H_1 & P_1 & \frac{1}{2}\end{Bmatrix}\begin{Bmatrix}lH_3 & lP_3 & q\\ P_3 & H_3 & \frac{1}{2}\end{Bmatrix}\\ &+\sum_{k} X_2\beta(k)\gamma_X(k)\theta(k)\begin{Bmatrix}P_1 & P_3 & k\\ lP_3 & lP_1 & \frac{1}{2}\end{Bmatrix}\begin{Bmatrix}H_3 & H_1 & k\\ lH_1 & lH_3 & \frac{1}{2}\end{Bmatrix}\Bigg],\end{aligned} \tag{A8}$$

where α, $\beta(x)$, $\gamma_D(k)$, $\gamma_X(k)$, D_1, D_2, X_1, and X_2 are defined in Eq. (A5).

Equation (A8) for $\mathfrak{M}_1$ is completely general in that the holes and particles can be either neutrons or protons providing there is the same number of protons and neutrons on each side of the two-hole–two-particle matrix element of Eq. (2). As pointed out above, even though Eq. (A8) appears more complicated than Eq. (5), it really represents a considerable simplification for numerically evaluating the two-hole–two-particle matrix element. The remaining 15 terms in the two-hole–two-particle matrix element can be obtained by making the changes indicated by Eq. (6) in Eq. (A8). For the special case of ^{208}Po which is calculated, $D_1=-H$, $D_2=M$, $X_1=-B$, and $X_2=W$ as indicated in Eq. (A3) above.

Equation (A8) was derived for the central force given in Eq. (A1). This expression is slightly more general than has been implied and could be used for some other types of interactions besides ones which contain a $V(r)$. For example, if $V(r)$ in Eq. (A1) was replaced by a multipole force of the form

$$\alpha_L r_1^L r_2^L P_L(\cos\theta_{12}),$$

the sums over k in Eq. (A8) above reduces to $k=L$ only and the Slater integrals $R^k(l_1l_2l_3l_4)$ are replaced by

$$\alpha_L\langle l_1|r^L|l_3\rangle\langle l_2|r^L|l_4\rangle .$$

†Supported in part by grants from the Atomic Energy Commission and the National Science Foundation.

[1]C. W. Ma and W. W. True, Phys. Rev. C 8, 2313 (1973).
[2]P. D. Barnes, E. R. Flynn, G. J. Igo, and D. D. Armstrong, Phys. Rev. C 1, 228 (1970).
[3]M. Rotenberg, R. Bivins, N. Metropolis, and J. K. Wooten, Jr., *The 3-j and 6-j Symbols* (Technology Press, Massachusetts, 1959).
[4]W. J. Treytl, E. K. Hyde, and T. Yamazaki, Nucl. Phys. A117, 481 (1968).
[5]T. Yamazaki, Phys. Rev. C 1, 290 (1970).
[6]L. H. Goldman, B. L. Cohen, R. A. Moyer, and R. C. Diehl, Phys, Rev. C 1, 1781 (1970).
[7]M. B. Lewis, Nucl. Data B5, 243 (1971).
[8]T. S. Bhatia, T. R. Canada, C. Ellegaard, J. Miller, E. Romberg, and P. D. Barnes, Bull. Am. Phys. Soc. 16, 1147 (1971).
[9]T. S. Bhatia, T. R. Canada, P. D. Barnes, R. Eisenstein, C. Ellegaard, and E. Romberg, Phys. Rev. Lett. 30, 496 (1973).
[10]W. W. True, C. W. Ma, and W. T. Pinkston, Phys. Rev. C 3, 2421 (1971).
[11]N. K. Glendenning and K. Harada, Nucl. Phys. 72, 481 (1965).
[12]G. Racah, Phys. Rev. 62, 438 (1942); 63, 367 (1943).
[13]J. D. Talman and W. W. True, Can. J. Phys. 42, 1081 (1964).